

A Novel Concept for Boiling Heat Transfer Enhancement

D. W. Zhou

Institute of Engineering Thermophysics, Chinese Academy of Sciences
B12, Zhongguancun, Haidian District, Beijing 100080, P.R. China, drdwzhou@hotmail.com

Abstract

The effect of bubble nucleation on boiling heat transfer enhancement has been investigated experimentally. Results show whether boiling heat transfer is enhanced or not depends directly on effective activation of vapor embryos on the heat transfer surface to initiate boiling. The mechanism of boiling heat transfer enhancement is analyzed and the influence factors of incipient boiling superheat are summarized. In light of bubble nucleation effect, the possible techniques for enhancing boiling heat transfer and eliminating boiling hysteresis are proposed and further developed as a principle to guide the research of boiling heat transfer enhancement.

1. Introduction

Boiling heat transfer has received an extensive attention because of its high heat transfer rate. However, most of the previous studies have been carried out to investigate the effects of such single or multi-ply factors as surface roughness [1], liquid temperature [2, 3], flow velocity [4, 5] and system pressure [6, 7] on boiling heat transfer, or to estimate the heat transfer performance through the established mathematical-physical model. Based on the presentation of the experimental data in the forms of $q'' \sim \Delta T_{\text{sat}}$ and/or $h \sim q''$, the former elucidates the macro-phenomenon of boiling heat transfer while the latter tries to explore the inherent mechanism of boiling heat transfer by comparing the numerical and experimental results. Consequently, it is assumed here that the primary objective of two above-mentioned methodologies is to study the boiling heat transfer only from the macroscopical point of view.

On the other hand, the heat transfer enhancement is an everlasting subject for both the researchers of heat transfer community of academia and technicians in industry, irrespectively of applied heat flux. Numerous investigations have been conducted experimentally and numerically and hence great achievements have been obtained. For single-phase convective heat transfer, Guo et al. [8] proposed a field synergy principle which can reveal the essence of heat transfer enhancement common to all enhancement methods. Subsequently, Tao and his co-workers [9, 10] extended this principle to elliptic fluid flow and other transport phenomena. This opens the way

to active control of convective heat transfer enhancement. To the knowledge of the present author, a similar unified theory for boiling heat transfer enhancement is difficult to find in literatures.

A new means for the data presentation of the experimental results was adopted in this study to investigate the effects of acoustic cavitation, CaCO_3 nanoparticles and fluid subcooling on boiling heat transfer. The purpose of the present study are threefold: the effect of bubble nucleation on boiling curves presented in terms of local wall temperature will be depicted; the mechanism of boiling heat transfer enhancement will be analyzed; and the techniques of boiling heat transfer enhancement will be provided to show the importance of this new concept.

2. Experimental Apparatus and Methods

The experimental apparatus and instrumentation are shown schematically in Fig. 1. The test chamber consisted of a cubical vessel made of stainless steel with inside dimensions of 200 mm \times 200 mm \times 230 mm. A horizontal copper tube with an electrical heating element inside passed through one pair of opposing walls 50 mm above the vessel base. Two viewing windows were installed on opposite sides of the vessel in parallel with the test tube for easy observation and taking pictures of the boiling heat transfer phenomena outside the test section. The vapor was condensed on the surface of a tap-water cooled condenser installed at the top of the vessel and then returned to the pool by gravity. Two

Nomenclature

C	concentration of nanometer particles, grams/lit	d	interior diameter of jet nozzle, m
h	heat transfer coefficient ($q''/(T_w-T_l)$), $W/(m^2K)$	L	sound source distance between the vibrator head and the central horizontal plane, m
P	sound source intensity, expressed by the power actually consumed by the ultrasonic vibrator, W	q''	heat flux, W/m^2
r/d	dimensionless radial distance from stagnation point	T_l	liquid temperature, K
T_{3-6}	local wall temperature on the bottom, top, (forward) side and backward (side) of the tube, K	T_w	arithmetic average of eight local wall temperatures, K
ΔT_{sat}	wall superheat (T_w-T_{sat}), K	$(\Delta T_{sat})_{ONB}$	incipient boiling superheat, K
ΔT_{sub}	fluid subcooling ($T_{sat} - T_l$), K	u	jet velocity, m/s
z/d	dimensionless nozzle-to-plate spacing		

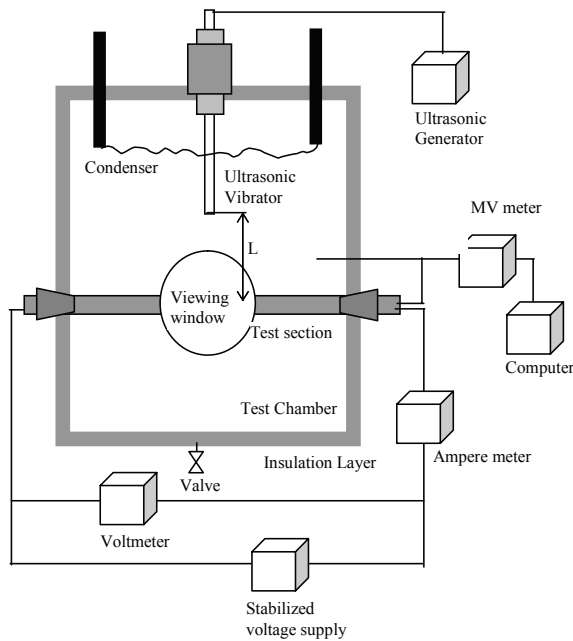


Fig. 1 Schematic layout of experimental setup

thermocouples located near the test section were used to measure the liquid pool temperature.

The details of the copper tube-heating element assembly are shown in Fig. 2. All test tubes were made of two copper tubes, the gap between which was fully filled with solder tin. The outer copper tube had an outer diameter of $\varnothing 20$ mm, an inner diameter of $\varnothing 16$ mm and a length of 152 mm and its outer surface was the test surface. The heater was inserted in the inner tube with a length of 138 mm, the outer and inner diameters of which were 15 mm and 12 mm, respectively. Eight nichrome-nisiloy thermocouples were arranged in eight $1.5 \text{ mm} \times 1.0 \text{ mm}$ grooves on the outer surface of the inner tube to measure the wall temperature shown in Fig. 2. The wall temperature was determined from the arithmetic average of the eight thermocouples after proper corrections of the conduction effect across the thickness of the copper tube.

The acoustical excitation was generated with an ultrasonic vibrator, which was operated by the electric current from an ultrasonic generator. The effect of the

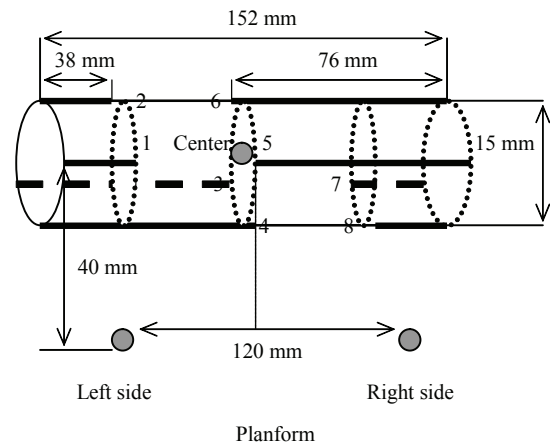


Fig. 2 Details of the electrically heated Test section assembly

acoustical field intensity on boiling heat transfer can be expressed in terms of three parameters: the ultrasonic source intensity P , the vibrator's location (left or right side or center) and the distance from the vibrator head to the horizontal plane containing the tube axis L (see Fig. 1), which is referred to as the sound source distance in this paper. More detailed experimental apparatus and procedure are described in [11, 12]. The input power was determined with a precision of 3.2%. The uncertainties in heat fluxes and heat transfer coefficients were estimated to be less than $\pm 5.5\%$ and $\pm 6.0\%$, respectively.

3. Results and Discussion

3.1 Boiling heat transfer enhancement from activated bubble nucleation

3.1.1 Acoustic cavitation

The effect of acoustic cavitation with sound source distance of $L= 40$ mm on local boiling curves obtained around the heated copper tube is presented in Fig. 3. You et al. [13] defined the superheat excursion at boiling inception as the maximum temperature difference (along a line of constant heat flux) between the surface

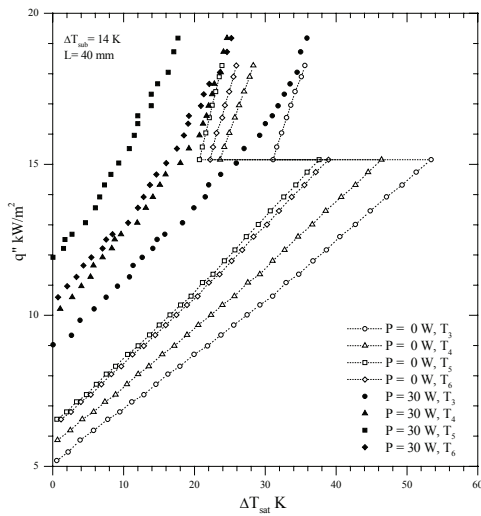
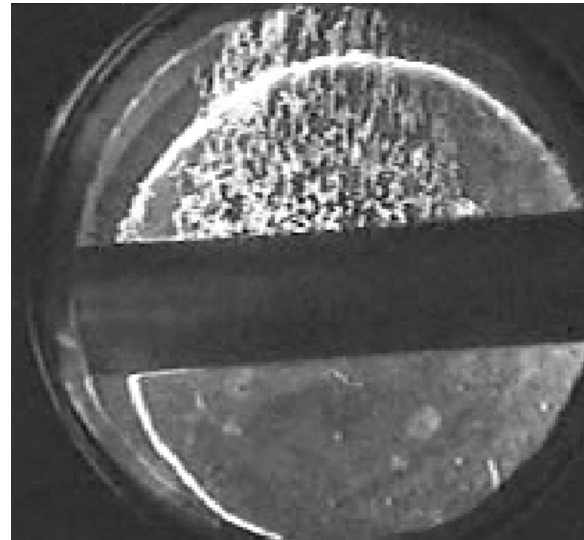


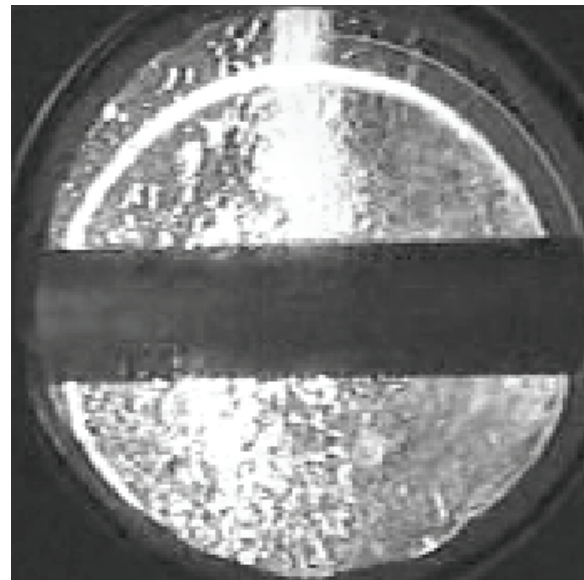
Fig. 3 Effect of sound source intensity on local wall temperature

temperature for increasing heat flux and that for decreasing heat flux. At given fluid subcooling of 14 K, boiling hysteresis with a maximum superheat excursion of 22.3 K occurred, irrespectively of the location of the thermocouple. However, as the sound source intensity is $P= 30$ W, boiling hysteresis disappears and the nucleate boiling curve shifts to the left of the corresponding pool curve without acoustic cavitation ($P= 0$ W) although the magnitude is different from each other. T_3 , T_4 , T_5 and T_6 represent the local wall temperature obtained from the bottom, side (forward), top and side (backward) of the tube shown in Fig. 2, respectively. Figure 3 shows that acoustic cavitation has much or less influence on four local wall temperatures around the tube and the wall temperature with higher heat transfer rate is in the following sequence: T_5 , T_6 , T_4 , and T_3 . It indicates that the copper tube obtained a minimum wall temperature on the top of the tube on which cavitation bubbles cluster impinges directly and a maximum wall temperature on the bottom of the tube where the impingement impact of cavitation bubbles cluster can be neglected. This causes the temperature difference around the tube at an identical applied heat flux increase because of the presence of acoustic cavitation, i.e., the nonuniformity of heat transfer rate at the same section of the tube increases.

We now discuss the reason for the above behavior. For pool boiling of the tube without acoustic cavitation, there is a higher heat transfer rate on the top of the tube than that on the bottom of the tube. The vapor embryos generated from the downside of the tube slide along the tube surface due to buoyancy and hence cause the boundary layer become thinner, contributing to higher high transfer rate there. When the vapor embryo arrive the upside of the tube, it is observed that: (i) the oncoming vapor embryos merge consecutively with the



(a) without acoustic cavitation ($P= 0$ W)



(b) with acoustic cavitation ($P= 60$ W)

Fig. 4 Bubble distributions around the tube surface (a) with and (b) without acoustic cavitation

local vapor embryos and hence much latent heat of vaporization is dissipated after departure from the surface of the heated tube; and (ii) the updraft bubbles disturb the boundary layer and hence heat is transferred through convection into the surrounding liquid. The combined influences of above-mentioned factors increase notably heat transfer rate on the top of the tube.

Figures 4a and 4b depict the bubble distributions around the tube surface during pool boiling with and without acoustic cavitation, respectively. Figure 4a presents the boiling behaviors of the copper tube without acoustic cavitation. It is concluded that no bubble is visible on the bottom of the tube. However, once acoustic

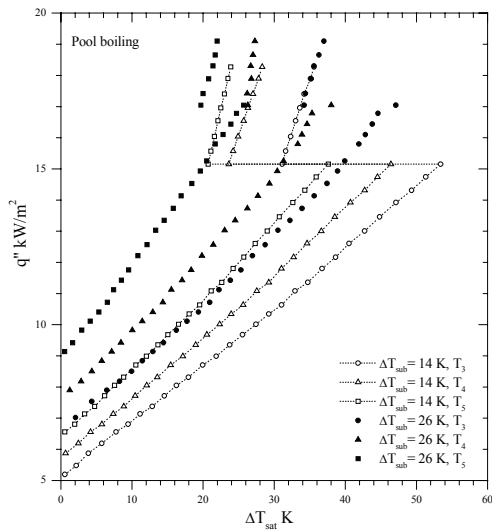


Fig. 5 Variation of local wall temperature with respect to fluid subcooling

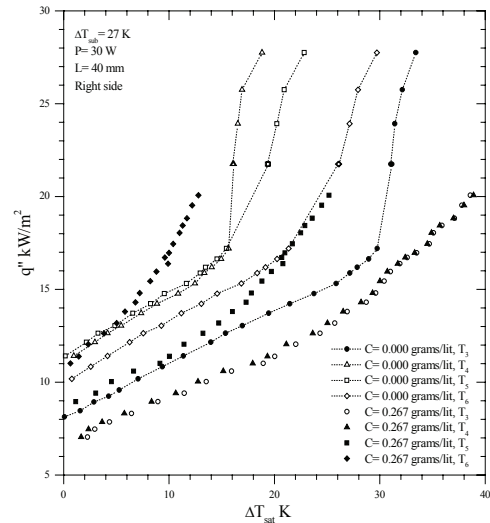


Fig. 6 Effect of nanoparticles on boiling heat transfer enhancement

cavitation shown in Fig. 4b with $P=60\text{ W}$ is generated, these cavitation bubbles excite consecutively vapor embryos harbored within the cavities on the tube surface by increasing or decreasing the pressure there. Therefore, bubbles that did not reach their critical radius are then fully activated by the cavitation bubbles [11]. Figure 4b shows that bubbles are visible not only on the top but also on the bottom of the tube. These bubbles activated by acoustic cavitation are clearly seen on the bottom of the tube from the videotape of the experiment. This in turn causes incipient boiling superheat decrease and eventually eliminate boiling hysteresis occurred on the smooth surface of the tube due to the use of highly-wetting liquid. On the other hand, the cavitation bubbles existed around the downside of the tube activated the liquid-gas interface within cavities, expediting the transportation of heat and mass there. It increases the actual areas for boiling heat transfer, which is believed to be another inherent mechanism of heat transfer enhancement by acoustic cavitation.

3.1.2 Fluid subcooling

Fluid subcooling influence on nucleate boiling heat transfer is another ambiguous academic problem remaining in this field. The experiments were carried out to investigate the fluid subcooling effect without acoustic cavitation on boiling heat transfer enhancement. Figure 5 presented the variation of local wall temperature obtained from the same section of the tube with respect to fluid subcooling. Independent of the location of the thermocouple, the pool boiling curves shift remarkably to the left with the increasing of fluid subcooling. That is to say, pool boiling heat transfer is enhanced. Although the applied heat flux at boiling inception increases, the incipient boiling superheat and superheat excursion

decrease. This is in agreement with the results reported by Ma and Bergles [5] and Zhou and Ma [4] for jet impingement boiling heat transfer. Figure 5 also shows that boiling heat transfer enhancement by fluid subcooling at the same section of the tube is different from each other. At $q''=1.52 \times 10^4\text{ W/m}^2$ for example, the decrease in the wall superheat at T_3 and T_5 between $\Delta T_{\text{sub}}=26\text{ K}$ and 14 K were 14 K and 16.2 K , respectively.

The afore-mentioned enhancement is believed to be caused mainly by two factors. With the increase of fluid subcooling, the thickness of the thermal boundary layer around the tube decreases, leading to an increase of convection heat transfer rate. Tong et al. [14] found that the surface tension of highly-wetting liquids usually increased with fluid subcooling, which makes the noncondensable gas dissolved in the working fluid be easy to be trapped. Both factors are helpful for greater cavities on the smooth heater surface to entrap vapor residues to initiate boiling. In other words, the ability for cavities on the heater surface to trap residues vapor increases and the corresponding size of cavities in which vapor residues were entrapped increases. Consequently, the boiling occurs at lower wall superheat and applied heat flux. The bubble nucleation within greater cavity size at boiling inception dissipates much heat to the surrounding fluid. Therefore, the boiling heat transfer is enhanced.

3.2 Boiling heat transfer reduction from suppressed bubble nucleation

3.2.1 The addition of nanoparticles

At fixed fluid subcooling of 27 K , the effect of CaCO_3 nanoparticles on local boiling curves obtained at same

section of the copper tube was presented in Fig. 6. The data are for $P=30\text{ W}$ and $L=40\text{ mm}$ where the ultrasonic vibrator locates on the right side of the test section. As shown in Fig. 6, the maximum temperature difference around the tube at fixed applied heat flux increases. Furthermore, the effect of acoustic cavitation on local wall temperature varied due to the presence of nanoparticles. As the CaCO_3 nanoparticles were added into the working fluid, the heated tube had a highest local wall temperature at T_6 rather than T_5 .

The CaCO_3 nanoparticles disperse uniformly in the working fluid under the impingement and disturbance of cavitation bubbles cluster. The uniformly-distributed nanoparticles counteract the generation and motion of cavitation bubbles, weakening acoustic cavitation influence there. It is assumed that little of nanoparticles deposit on the downside of the tube due to gravity, resulting in a weak influence on local wall temperature T_3 . The combined effect of two above-mentioned factors decreases the numbers of nucleation embryos, contributing to a low heat transfer rate of nucleate boiling. The corresponding boiling curve shifts to the right. It should be noted here that the size of nanoparticles (about 80-100 nm) is much less than that of cavities in which vapor embryos will be activated to initiate boiling. As a result, more nanoparticles deposit on the upside of the heated tube under the impingement and disturbance of acoustic cavitation cluster. Due to the deposition of nanoparticles, the surface roughness of the tube decreases. It would then require elevated applied heat flux to activate vapor embryos at the remaining smaller cavities prior to boiling inception, i.e., the presence of nanoparticles suppresses bubble nucleation within the cavities on the surface of the heated tube. At the same test conditions, heat is dissipated only by convection rather than by latent heat of vaporization and the mode of heat transfer is single-phase convection. Consequently, the incipient boiling superheat increases and the corresponding local boiling curve shifts to the right. This has been verified by the data indicated by thermocouple of T_5 shown in Fig. 6.

3.2.2 High jet exit velocity impinged at the stagnation point

Zhou and Ma confirmed [4] that, as the exit velocity of circular jet did not exceed 10 m/s, both the pool and impingement nucleate boiling curves at the same subcooling condition were well correlated with an equation. However, as shown in Fig. 7, the impingement boiling curve obtained at the stagnation point with higher jet exit velocity of 11.36 m/s shifts to the right of the low velocity curve. Ma and Bergles [5] reported this phenomenon, yet did not give any explanation for it.

Zhou and Ma [4] concluded that the pressure distribution controlled the local saturation conditions along the impingement plate surface. At the stagnation point, impingement velocity sharply decreases to zero while the pressure increases correspondingly to a maximum value. This in turn causes the saturation temperature of the working fluid increase. Therefore, the

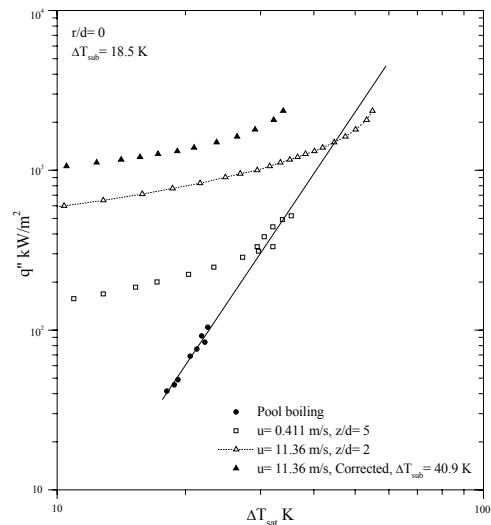


Fig. 7 Effect of jet exit velocity on the stagnation boiling curve

boiling curve with higher jet exit velocity and the corresponding fluid subcooling were corrected in terms of the elevated saturation temperature. As can be seen in Fig. 7, the corrected fluid subcooling is increased sharply from 18.5 K to 40.9 K and the corresponding boiling curve is located to the left of the original boiling curve.

We now analyze the displacement of impingement nucleate boiling curve in light of bubble generation behavior. As the jet impinges the heater surface, a local thinner thermal boundary layer at the impingement zone is available due to its normal flow, contributing to higher heat transfer rate there. Since the working fluid (R113) has low surface tension and small contact angle, they flood all but the smallest cavities on the heat transfer surface (smooth constantan foil), depleting vapor embryos needed for boiling inception [15]. The vapor embryos can not be activated due to unavailable residual gas within greater cavities. The heater surface dissipates the heat only by conduction and convection prior to bubble nucleation. Only when the applied heat flux increases to a certain value, vapor embryos within cavities on the heater surface can generate, grow up and separate. Thus, the boiling commences. Since the effects of jet exit velocity cannot reach the interior surface of these cavities, the incipient boiling superheat is irrelevant to jet exit velocity. But, as the jet with higher exit velocity of 10 m/s impinges at the stagnant point, it is inferred that the bubble nucleation occurred within the cavities on the heater surface are spoilt by the impingement liquid. The high-speed flowing fluid dissipates much heat by convection and more latent heat of vaporization by bubble nucleation, resulting in significant increase in heat transfer rate. It should be stressed that vapor embryos could be activated in this

case but could not grow up easily. This maintains a low wall superheat although the applied heat flux reaches a higher level. As the heat flux is increased further, the heat transfer mode on the impingement surface converts gradually from single-phase forced convection into fully-developed nucleate boiling. It seems that the suppression effect of jet velocity on bubble nucleation within the cavities is more sensible at higher jet exit velocity. As the jet exit velocity exceeds 10 m/s, the displacement of impingement boiling curve obtained at the stagnation point occurs in comparison with that of the low velocity with an identical fluid subcooling.

As the highly-wetting liquid is used as the working fluid, both acoustic cavitation and impinging jet can eliminate boiling hysteresis, but in different way. Acoustic cavitation activates more vapor embryos below the critical radius to boil while the jet with higher jet exit velocity of 10 m/s impinging at the stagnation point suppresses the bubble nucleation. It is believed whether or not vapor embryos are activated not only indicates the heat transfer mode on the heater surface, but also determines the slope and location of the boiling curve. Consequently, it is concluded here that boiling heat transfer enhancement results from the activated bubble nucleation and vice versa.

4 Controlling techniques for enhancing boiling heat transfer

4.1 Influence factors of incipient boiling superheat

From previous literatures, we may summarize the main factors which influence incipient boiling superheat as follow: thermal properties of the liquid coolant and wall [16] and the corresponding contact angle [14], thermal history of the wall (i.e., surface aging) and the heating procedure [17], heater size and orientation [18], system pressure [6, 7, 19], fluid subcooling [2, 3, 17], surface roughness [1] and additional field (such as gravitational field [6, 20], electric field [21, 22], acoustic field [23, 11] and magnetic field [24]), etc. Once the working fluid and the material of the heat transfer surface are selected, the contact angle between them is determined. Generally speaking, the thermal behavior at boiling inception is influenced not only by the surface condition at the moment of boiling inception but also by the thermal processes associated with the surface before this moment. Thus, an experimental procedure of boiling heat transfer proposed recently by Zhou et al. [17] should be rigorously performed to eliminate the effects of such factors as surface aging, noncondensable gas and the heating procedure on boiling heat transfer, especially for the case of highly-wetting liquid.

For a clean heat transfer surface, the incipient boiling superheat is only related with the system pressure, fluid subcooling, surface roughness and the additional fields after the above-mentioned factors are determined. Figure 8 presented these factors influences on incipient boiling superheat. Since such factors as fluid subcooling, surface

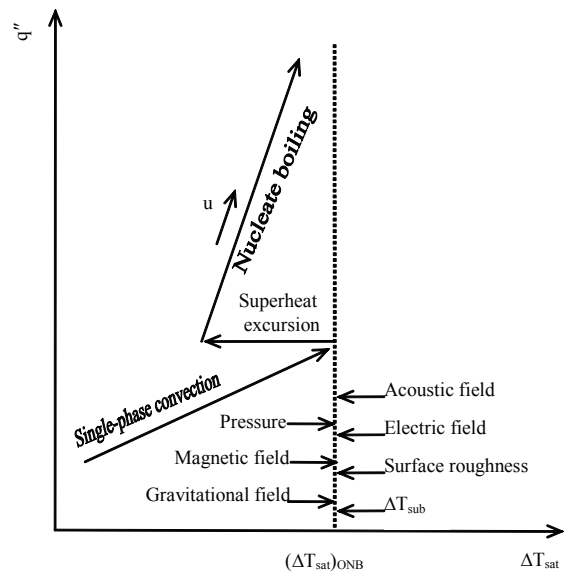


Fig. 8 Effects of various factors on incipient boiling superheat

roughness, electric field and acoustic field can activate vapor embryos on the heater surface, the incipient boiling superheat decreases with the increased intensity of these factors. On the contrary, the bubble nucleation process is suppressed with the increased intensity of system pressure, magnetic field and gravitational field. Figure 8 also shows the fluid velocity effect on incipient boiling superheat. It is believed that low fluid velocity has a negligible influence on incipient boiling superheat and only pushes the high heat flux regime of boiling curve to higher heat fluxes. This has been verified by the experimental data of Yin and Abdelmessih [25] for an R11 flow boiling and Zhou et al. [17] for R113 impingement boiling.

The above analysis shows that the incipient boiling superheat is closely related with the thermal and mechanical properties of the liquid coolant and wall, the experimental procedure, system pressure, fluid subcooling, surface roughness and the additional field. It should be noted here that the first two factors have been determined prior to the experimental runs. According to the analysis in section 3, it is concluded that the remainder factors influence the incipient boiling superheat by changing the system pressure, saturation temperature of the working fluid, surface roughness, or fluid subcooling. This in turn indicates that the incipient boiling superheat can be increased or decreased by changing directly or indirectly these factors.

4.2 Possible technique to enhance boiling heat transfer

Extensive consideration has been given to boiling heat transfer enhancement. The possible techniques for enhance boiling heat transfer prior to 1998 have been reviewed by Rohsenow [26] in detail. However, as we

know from the afore-mentioned analysis, once vapor embryos are effectively activated to initiate boiling, the boiling heat transfer is enhanced, irrespectively of the techniques of bubble nucleation. On the contrary, the boiling heat transfer is reduced while bubble nucleation is suppressed to initiate boiling. Due to the suppression of bubble nucleation by the Lorentz force, Wagner and Lykoudis [24] and Takahashi et al. [27] found that the boiling heat transfer was reduced with increasing the magnetic flux density in comparison with the case of non-magnetic field. Consequently, in order to actively develop the techniques of boiling heat transfer enhancement, we should understand thoroughly the potential techniques which can activate vapor embryos to initiate boiling.

Probably the most challenging task of performing the principle is to develop boiling heat transfer enhancement techniques at the guidance of the principle. However, such work is now underway in the authors' group. Several examples are presented for illustration. Fukusako et al. [28] confirmed that porous medium could contain more dissolved noncondensable gases than a smooth surface. Thus, it would lead to an increase of nucleation nuclei density. For a heated horizontal copper tube embedded in a porous medium, Zhou et al. [12] verified that the boiling heat transfer was enhanced due to the presence of porous medium. Since acoustic cavitation can activate residual gas harbored within the cavities on the heat transfer surface, the experimental data of Zhou et al. [11] indicated that the boiling heat transfer was enhanced notably while the acoustic source intensity exceeded a certain value. Zhou [29] also investigated the effect of copper nanofluid on boiling heat transfer of the horizontal tube and concluded that the deposition of copper nanoparticles on the heater surface suppressed the bubble nucleation, leading to reduction in boiling heat transfer.

4.3 Possible techniques to eliminate boiling hysteresis

Due to unfavorable influence, the boiling hysteresis must be eliminated in its practical applications. Therefore, options for eliminating boiling hysteresis and enhancing boiling heat transfer have been considered. The mechanism of boiling hysteresis reported by Zhou et al. [17] and carried out in section 3 showed that the occurrence of boiling hysteresis was primarily attributed to the delayed nucleation of vapor embryos. It occurs due to the smooth heater surface, and is exacerbated by the small surface tension of highly-wetting liquid. The basic characteristic of boiling hysteresis is its higher incipient boiling superheat prior to boiling inception. As a result, the fundamental way to eliminate boiling hysteresis is to activate effectively vapor embryos so as to initiate boiling at normal wall superheat. Since boiling hysteresis is accompanied with lower heat transfer rates prior to boiling inception, it implies that the elimination of boiling hysteresis is an extreme case of boiling heat transfer enhancement.

It is believed that the possible techniques to enhance boiling heat transfer can also be utilized to eliminate

boiling hysteresis. For example, Cooper [21] and Zaghoudi and Lallemand [22] found that the uses of electric field enhanced boiling heat transfer and eliminated boiling hysteresis. Zhou et al. [11] reported a similar result for an acoustic field. Joudi and James [7] observed the incipient boiling characteristics at atmospheric and subatmospheric pressures, and found that many nucleation sites on the surface would be active at decreased pressures, leading to disappearance of boiling hysteresis. These examples indicate that the normal activation of vapor embryos occurs due to the presence of electric field, acoustic field and decreased pressures, leading to boiling heat transfer enhancement.

Considerable attention has been given to either altering the surface or attaching it to a heat sink. Information on reentrant cavity published prior to 1997 was summarized by Bergles [30]. Recently, with the use of compound surface and "doubly reentrant" cavity on the boiling surface respectively, Liang and Yang [31] and Reed and Mudawar [32] eliminated successfully boiling hysteresis because vapor embryos were easily activated on the two kinds of surfaces.

5. Conclusions

The most important findings of this study are:

- (1) Boiling heat transfer enhancement results from effective bubble nucleation on the heat transfer surface at normal wall superheat and vice versa.
- (2) In light of the bubble nucleation effect on boiling heat transfer enhancement, a new principle is proposed to guide the research of enhancing boiling heat transfer and eliminating boiling hysteresis. Some typical examples are presented in the paper for illustration.

Acknowledgements

The assistance and valuable suggestions of Professor Arthur E. Bergles of Massachusetts Institute of Technology (Cambridge) is highly appreciated.

References

- [1] S.K. Roy Chowdhury, R. H. S. Winterton, Surface effects in pool boiling, *International Journal of Heat Mass Transfer*, 28 (3) (1985) 1881-1889.
- [2] R.L. Judd, H.JR. Merte, Evaluation of nucleate boiling heat flux predictions at varying levels of subcooling and acceleration, *International Journal of Heat Mass Transfer*, (15) (1972) 1075-1096.
- [3] V.H. Del Valle M, Kenning D B R, Subcooled flow boiling at high flux, *International Journal of Heat Mass Transfer*, 28 (6) (1985) 1907-1920.
- [4] D. W. Zhou, C. F. Ma, Local jet impingement boiling heat transfer with R113, *Heat and Mass Transfer*, 40 (6) (2004) 91-100.

- [5] C. F. Ma, A. E. Bergles, Jet impingement nucleate boiling, *International Journal of Heat Mass Transfer*, 29 (2) (1986) 1095-1100.
- [6] J. S. Turton, The effects of pressure and acceleration on the pool boiling of water and acetone 11, *International Journal of Heat Mass Transfer*, (11) (1968) 1295-1303.
- [7] K.A. Joudi, D.D. James, Incipient boiling characteristic at atmospheric and sub-atmospheric pressure, *Journal of Heat Transfer*, (99) (1977) 398-404.
- [8] Z. Y. Guo, D. Y. Li, B. X. Wang, A novel concept for convective heat transfer enhancement, *International Journal of Heat Mass Transfer*, (41) (1998) 2221-2225.
- [9] W. Q. Tao, Z. Y. Guo, B. X. Wang, Field synergy principle for enhancing convective heat transfer- its extension and numerical verifications, *International Journal of Heat Mass Transfer*, (45) (2002) 3849-3856.
- [10] W. Q. Tao, Y. L. He, Q. W. Wang, Z. G. Qu, F. Q. Song, A unified analysis on enhancing single phase convective heat transfer with field synergy principle, *International Journal of Heat Mass Transfer*, (45) (2002) 4871-4879.
- [11] D. W. Zhou, D. Y. Liu, X. G. Hu, C. F. Ma, Effect of acoustic cavitation on boiling heat transfer, *Experimental Thermal Fluid Science*, 26 (10) (2002) 931-938.
- [12] D. W. Zhou, D. Y. Liu, P. Cheng, Boiling heat transfer characteristics from a horizontal tube embedded in a porous medium with acoustic excitation, *Journal of Enhanced Heat Transfer*, (11) (3) (2004) 91-100.
- [13] S. M. You, T. W. Simon, A. Bar-Cohen, W. Tong, Experimental investigation of nucleate boiling incipience with a highly wetting dielectric fluid (R113), *International Journal of Heat Mass Transfer*, (33) (1990) 105-117.
- [14] W. Tong, A. Bar-Cohen, S. M. You, Contact angle effects on boiling incipience of highly-wetting liquids, *International Journal of Heat Mass Transfer*, (33) (1) (1990) 91-100.
- [15] A. Bar-Cohen, T. W. Simon, Wall superheat excursions in the boiling incipience of dielectric fluids, *Heat Transfer Engineering*, 9(3) (1988) 19-31.
- [16] K. A. Joudi, D. D. James, Surface contamination, rejuvenation, and the reproducibility of results in nucleate pool boiling. *Journal of Heat Transfer*, 103 (8) (1981) 453-460.
- [17] D. W. Zhou, C. F. Ma, J. Yu, Boiling hysteresis of impinging circular submerged jets with highly wetting liquids, *International Journal of Heat and Fluid Flow*, 25 (1) (2004) 81-90.
- [18] K. N. Rainey, S. M. You, Effects of heater size and orientation on pool boiling heat transfer from microporous coated surfaces, *International Journal of Heat Mass Transfer*, (44) (2001) 2589-2599.
- [19] A. E. Bergles, W. M. Rohsenow, The determination of forced convection surface boiling heat transfer, *Journal of Heat Transfer*, 86 (8) (1964) 365-370.
- [20] H. S. Lee, H. Merte, F. Chiamonte, Pool boiling curve in microgravity, *Journal of Thermophysics and Heat Transfer*, 11 (2) (1997) 216-222.
- [21] P. Cooper, EHD enhancement of nucleate boiling, *Journal of Heat Transfer*, (112) (1990) 458-464.
- [22] M. C. Zaghoudi, M. Lallemand, Electric Field Effects on Pool Boiling, *Journal of Enhanced Heat Transfer*, 9(5-6) (2002) 187-208.
- [23] K.A. Park, A. E. Bergles, Ultrasonic enhancement of saturated and subcooled pool boiling, *International Journal of Heat Mass Transfer*, (31) (1988) 664-667.
- [24] L. Y. Wagner, P. S. Lykoudis, Mercury pool boiling under the influence of a horizontal magnetic field, *International Journal of Heat Mass Transfer*, 24 (4) (1981) 635-643.
- [25] S. T. Yin, A. H. Abdelmessih, Prediction of incipient flow boiling from a uniformly heated surface. *Nuclear, Solar, and Process Heat Transfer-St. Louis*, (73) (1977) 236-242.
- [26] W. M. Rohsenow, Boiling, in: W.M. Rohsenow, J. P. Hartnett, Y. I. Chi (Eds.), *Handbook of Heat Transfer*, third ed., McGraw-Hill, New York, 1998, pp. 13.1-13.76.
- [27] O. Takahashi, M. Nishida, N. Takenaka, I. Michiyoshi, Pool boiling heat transfer from horizontal plane heater to mercury under magnetic field, *International Journal of Heat Mass Transfer*, (23) (1980) 27-36.
- [28] S. Fukusako, T. Komoriya, N. Seki, An experimental study of transition and film boiling heat transfer in liquid-saturated porous bed, *Journal of Heat Transfer*, (108) (1986) 117-124.
- [29] D. W. Zhou, Heat transfer enhancement of copper nanofluid with acoustic cavitation, *International Journal of Heat Mass Transfer*, (47) (14-16) (2004) 3109-3117.
- [30] A. E. Bergles, Heat transfer enhancement- The encouragement and accommodation of high heat fluxes, *Journal of Heat Transfer*, (119) (2) (1997) 8-18.
- [31] H. S. Liang, W. J. Yang, Nucleate pool boiling heat transfer in a highly wetting liquid on micro-graphite fiber composite surfaces, *International Journal of Heat Mass Transfer*, 41 (13) (1998) 1993-2000.
- [32] R. J. Reed, I. Mudawar, Elimination of boiling incipience temperature drop in highly wetting fluids using spherical contact with a flat surface, *International Journal of Heat Mass Transfer*, (42) (1999) 2439-2454.